Nucleon Transversity Distribution in the Continuum and Physical Mass Limit from Lattice QCD

Fei Yao,[2] Lisa Walter,[3] Jiunn-Wei Chen,[4,5] Jun Hua,[6,7] Xiangdong Ji,[8] Luchang Jin,[9,10] Sebastian Lahrtz,[3] Lingquan Ma,[2] Protick Mohanta,[2,11] Andreas Schäfer,[3] Hai-Tao Shu,[3] Yushan Su,[8] Peng Sun,[12,13,*] Xiaonu Xiong,[1,†] Yi-Bo Yang,[14–17] and Jian-Hui Zhang[18,2]

(Lattice Parton Collaboration)

[1]*School of Physics, Central South University, Changsha 418003, China*
[2]*Center of Advanced Quantum Studies, Department of Physics, Beijing Normal University, Beijing 100875, China*
[3]*Institut für Theoretische Physik, Universität Regensburg, D-93040 Regensburg, Germany*
[4]*Department of Physics, Center for Theoretical Physics, and Leung Center for Cosmology and Particle Astrophysics, National Taiwan University, Taipei 10617, Taiwan*
[5]*Physics Division, National Center for Theoretical Sciences, Taipei 10617, Taiwan*
[6]*Guangdong Provincial Key Laboratory of Nuclear Science, Institute of Quantum Matter, South China Normal University, Guangzhou 510006, China*
[7]*Guangdong-Hong Kong Joint Laboratory of Quantum Matter, Southern Nuclear Science Computing Center, South China Normal University, Guangzhou 510006, China*
[8]*Department of Physics, University of Maryland, College Park, Maryland 20742, USA*
[9]*Physics Department, University of Connecticut, Storrs, Connecticut 06269-3046, USA*
[10]*RIKEN BNL Research Center, Brookhaven National Laboratory, Upton, New York 11973, USA*
[11]*School of Physical Sciences, National Institute of Science Education and Research, HBNI, Odisha 752050, India*
[12]*Institute of Modern Physics, Chinese Academy of Sciences, Lanzhou, Gansu Province 730000, China*
[13]*Department of Physics and Institute of Theoretical Physics, Nanjing Normal University, Nanjing, Jiangsu 210023, China*
[14]*CAS Key Laboratory of Theoretical Physics, Institute of Theoretical Physics, Chinese Academy of Sciences, Beijing 100190, China*
[15]*School of Fundamental Physics and Mathematical Sciences, Hangzhou Institute for Advanced Study, UCAS, Hangzhou 310024, China*
[16]*International Centre for Theoretical Physics Asia-Pacific, Beijing/Hangzhou, China*
[17]*University of Chinese Academy of Sciences, School of Physical Sciences, Beijing 100049, China*
[18]*School of Science and Engineering, The Chinese University of Hong Kong, Shenzhen 518172, China*

(Received 28 July 2022; revised 17 October 2023; accepted 17 November 2023; published 26 December 2023)

We report a state-of-the-art lattice QCD calculation of the isovector quark transversity distribution of the proton in the continuum and physical mass limit using large-momentum effective theory. The calculation is done at four lattice spacings $a = \{0.098, 0.085, 0.064, 0.049\}$ fm and various pion masses ranging between 220 and 350 MeV, with proton momenta up to 2.8 GeV. The result is nonperturbatively renormalized in the hybrid scheme with self-renormalization, which treats the infrared physics at large correlation distance properly, and extrapolated to the continuum, physical mass, and infinite momentum limit. We also compare with recent global analyses for the nucleon isovector quark transversity distribution.

DOI: 10.1103/PhysRevLett.131.261901

Introduction.—Parton distribution functions (PDFs) characterize the internal structure of hadrons in terms of the number densities of their quark and gluon constituents. They are crucial inputs for interpreting the experimental data collected at high-energy colliders such as the LHC. At leading-twist accuracy, there exist three quark PDFs: the unpolarized, the helicity, and the transversity PDF [1]. Among them, the transversity PDF describes the correlation between the transverse polarizations of the nucleon and its quark constituents, thus, plays an important role in describing the transverse spin structure of the nucleon [2]. In contrast to the unpolarized and helicity PDFs, the transversity PDF is much less constrained from experiments. This is because it is a chiral-odd quantity and has to couple to another chiral-odd quantity, such as the chiral-odd

Published by the American Physical Society under the terms of the Creative Commons Attribution 4.0 International license. Further distribution of this work must maintain attribution to the author(s) and the published article's title, journal citation, and DOI. Funded by SCOAP³.

fragmentation or distribution function, in order to be measurable experimentally [3–5]. Currently, our knowledge of the transversity PDF mainly comes from measuring certain spin asymmetries in semi-inclusive deep-inelastic scattering or electron-positron annihilation to a hadron pair and Drell-Yan processes [6,7]. Based on these data, various global analyses of the transversity PDF have been performed [6,8–18]. Such analyses are expected to be greatly improved when more accurate data are accumulated at ongoing and future experiments at, e.g., the JLab 12 GeV upgrade and the Electron-Ion Collider (EIC).

On the other hand, recent theoretical developments [19–24] have allowed us to calculate and fit the Bjorken x dependence of PDFs from first-principle lattice QCD. Such calculations are particularly important for quantities like the nucleon transversity PDF which are hard to extract from experiments. In the past few years, several lattice calculations [25–27] of the nucleon transversity PDF have been carried out using either the large-momentum effective theory (LaMET) [20,21,28] or the short-distance expansion (pseudo-PDF) [24]. However, they were all done at a single lattice spacing, while a reliable extrapolation to the continuum is required to make a comparison with experimental measurements. Moreover, the nonperturbative renormalization used in these calculations has been shown to suffer from undesired infrared (IR) effects arising from the improper renormalization at long distances [29]. Therefore, it is highly desirable to obtain a reliable prediction that uses a proper renormalization and is valid in the continuum and physical mass limit. This is the purpose of the present work.

In this Letter, we present a state-of-the-art lattice calculation of the isovector quark transversity PDF $\delta u(x) - \delta d(x)$ of the proton, using the LaMET approach. The lattice matrix elements of the transversity quasi-PDF are calculated at four lattice spacings $a = \{0.098, 0.085, 0.064, 0.049\}$ fm and various pion masses ranging between 220 and 350 MeV, with proton momenta up to 2.8 GeV. The result is nonperturbatively renormalized in the hybrid scheme [29] with self-renormalization [30] proposed recently, which is a viable IR-safe renormalization approach, and extrapolated to the continuum, physical mass, and infinite momentum. We also make a comparison between our results and recent global analyses on the isovector quark transversity PDF of the proton [6,18].

Theoretical framework.—The leading-twist quark transversity PDF $\delta q(x)$ of the proton is defined as [2]

$$\delta q(x,\mu) = \int \frac{d\xi^-}{4\pi} e^{-ixP^+\xi^-} \langle PS_\perp | \bar{\psi}(\xi^-)\gamma^+\gamma^\perp\gamma_5 \times \mathcal{W}[\xi^-,0]\psi(0)|PS_\perp\rangle, \quad (1)$$

where $|PS_\perp\rangle$ denotes a transversely polarized proton with momentum P along the z direction and polarization $S_\perp$ along the transverse direction, x is the momentum fraction carried by the quark, μ is the renormalization scale in the $\overline{\text{MS}}$ scheme, $\xi^\pm = (\xi^t \pm \xi^z)/\sqrt{2}$ are light-cone coordinates, and $\mathcal{W}[\xi^-,0] = \mathcal{P}\exp[ig\int_{\xi^-}^0 du\, n\cdot A(un)]$ is the gauge link along the light-cone direction ensuring gauge invariance of the nonlocal quark bilinear correlator.

According to LaMET, we can extract the transversity PDF from the following transversity quasi-PDF on the lattice:

$$\delta\tilde{q}(x,P_z,1/a) = \int \frac{dz}{2\pi} P_z e^{ixzP_z} \bar{h}(z,P_z,1/a),$$
$$\bar{h}(z,P_z,1/a) = \frac{1}{2P_0}\langle PS_\perp|\bar{\psi}(z)\gamma^t\gamma^\perp\gamma_5\mathcal{W}[z,0]\psi(0)|PS_\perp\rangle, \quad (2)$$

where $\bar{h}(z,P_z,1/a)$ is the equal-time or quasi-light-front (quasi-LF) correlation that can be calculated directly on the lattice and a denotes the lattice spacing. Throughout this Letter, we take the flavor combination $\delta\tilde{u}(x) - \delta\tilde{d}(x)$ to eliminate disconnected contributions.

The bare quasi-LF correlation above contains both linear and logarithmic ultraviolet (UV) divergences, which need to be removed by a proper nonperturbative renormalization. Various approaches have been suggested and implemented in the literature [31–36]. However, they all suffer from the problem that the renormalization factor introduces undesired nonperturbative contributions distorting the IR behavior of the original quasi-LF correlation. This is avoided in the so-called hybrid scheme [29], where one separates the quasi-LF correlations at short and long distances and renormalize them separately. At short distances, the renormalization is done by dividing by the same hadron matrix element in the rest frame, as is done in the ratio scheme [34]; at long distances, one removes the UV divergences of the quasi-LF correlation only, which are determined by the so-called self-renormalization [30] through fitting the bare matrix elements at multiple lattice spacings to a physics-dictated functional form. The renormalized quasi-LF correlation then takes the following form:

$$\tilde{h}_R(z,P_z) = \frac{\tilde{h}(z,P_z,1/a)}{\tilde{h}(z,P_z=0,1/a)}\theta(z_s-|z|) + \eta_s\frac{\tilde{h}(z,P_z,1/a)}{Z_R(z,1/a)}\theta(|z|-z_s), \quad (3)$$

where we have introduced an additional normalization $\tilde{h}(z,P_z,1/a) = \bar{h}(z,P_z,1/a)/\bar{h}(z=0,P_z,1/a)$ to cancel lattice artifacts. As a result, our Fourier transformed momentum distribution will give 1 rather than the nucleon isovector tensor charge g_T upon integration. Our $g_T = 1.018(68)$ is extracted from the local matrix elements and is consistent with the Mainz19, FLAG21 result [37,38] (see Supplemental Material [39] for the details of extracting nucleon isovector tensor charge g_T, which includes Refs. [40–42]). In Eq. (3), z_s is introduced to separate the short and long distances and has to lie in the

perturbative region. $Z_R(z, 1/a)$ denotes the renormalization factor extracted from the self-renormalization procedure using the same transversity three-point correlator in the rest frame. Details are given in Supplemental Material [39]. We have included a factor η_s which is similar to a scheme conversion factor and determined by requiring continuity of the renormalized quasi-LF correlation at $z = z_s$. Of course, one needs to check the stability of the final result with respect to the choice of z_s. We vary z_s in a certain perturbative range and include the difference in the systematic uncertainties. Note that all singular dependence on a has been canceled in the above equation so that $\tilde{h}_R$ is independent of a (up to some finite discretization effects).

After performing a Fourier transform to momentum space, we can match the transversity quasi-PDF to the transversity PDF through the following perturbative matching:

$$\delta\tilde{q}(x, P_z) = \int_{-1}^{1} \frac{dy}{|y|} C\left(\frac{x}{y}, \frac{\mu}{yP_z}\right) \delta q(y, \mu) + \mathcal{O}\left(\frac{\Lambda^2_{\rm QCD}}{(xP_z)^2}, \frac{\Lambda^2_{\rm QCD}}{[(1-x)P_z]^2}\right), \quad (4)$$

where C is the perturbative matching kernel whose explicit expression to $\mathcal{O}(\alpha_s)$ is given in Supplemental Material [39] (which includes Refs. [43,44]). The transversity at negative y can be interpreted as the antiquark transversity via the relation $\delta\tilde{q}(y, \mu) = -\delta q(-y, \mu)$. $\mathcal{O}\{[\Lambda^2_{\rm QCD}/(xP_z)^2], (\Lambda^2_{\rm QCD}/[(1-x)P_z]^2)\}$ denotes higher-twist contributions suppressed by the nucleon momentum P_z.

Lattice calculation.—To improve the signal-to-noise ratio of calculations with high-momentum nucleon states, we employ the momentum smearing source technique [45]. Besides, we apply two-step APE smearing to further improve the signal. We also use the sequential source method with fixed sink to calculate the quark three-point correlator, as illustrated in Fig. 1. In order to perform the continuum and chiral extrapolation, we use six different lattice ensembles generated by the CLS Collaboration [46] with lattice spacing $a = \{0.098, 0.085, 0.064, 0.049\}$ fm and pion masses ranging between 354 and 222 MeV. For each ensemble, we calculate several source-sink separations with hundreds to thousands of measurements among 500 gauge configurations (for X650, it is 1500 because the autocorrelation time is larger for this rather coarse lattice). Details of the lattice setup and parameters are collected in Table I.

The bare matrix elements are calculated with the nucleon carrying different spatial momenta on each ensemble: $P_z = \{1.84, 2.37, 2.63\}$ GeV on X650, $P_z = \{1.82, 2.27, 2.73\}$ GeV on H102, $P_z = 1.82$ GeV on H105 and C101, $P_z = \{1.62, 2.02, 2.43, 2.83, 3.24\}$ GeV on N203, and $P_z = \{2.09, 2.62\}$ GeV on N302. We also calculate the zero-momentum bare matrix elements for each ensemble, which provide the renormalization factor at short distance and the inputs to extract the renormalization factor at long distance through self-renormalization.

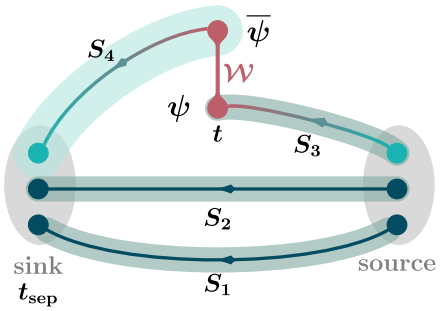

FIG. 1. Illustration of the sequential source method. The time direction is from source to sink. Propagators $S_{1,2}$ are combined to construct the sequential source. The inversion with the sequential source gives propagator S_4. S_4, S_3, gauge link $\mathcal{W}$, and necessary projectors are assembled to get the three-point correlator.

To extract the ground state matrix element, we decompose the two-point correlator $C^{\rm 2pt}(P_z, t_{\rm sep})$ and three-point correlator $C^{\rm 3pt}_\Gamma(P_z, t, t_{\rm sep})$ (with $\Gamma = \gamma^t\gamma^\perp\gamma_5$) as in [48]:

$$\begin{aligned} C^{\rm 2pt}(P_z, t_{\rm sep}) &= |\mathcal{A}_0|^2 e^{-E_0 t_{\rm sep}} + |\mathcal{A}_1|^2 e^{-E_1 t_{\rm sep}} + \cdots, \\ C^{\rm 3pt}_\Gamma(P_z, t, t_{\rm sep}) &= |\mathcal{A}_0|^2 \langle 0|O_\Gamma|0\rangle e^{-E_0 t_{\rm sep}} \\ &\quad + |\mathcal{A}_1|^2 \langle 1|O_\Gamma|1\rangle e^{-E_1 t_{\rm sep}} \\ &\quad + \mathcal{A}_1\mathcal{A}_0^* \langle 1|O_\Gamma|0\rangle e^{-E_1(t_{\rm sep}-t)} e^{-E_0 t} \\ &\quad + \mathcal{A}_0\mathcal{A}_1^* \langle 0|O_\Gamma|1\rangle e^{-E_0(t_{\rm sep}-t)} e^{-E_1 t} + \cdots, \end{aligned} \quad (5)$$

where $\langle 0|O_\Gamma|0\rangle = \tilde{h}(z, P_z, 1/a)$ is the ground state matrix element and t denotes the insertion time of O_Γ. The ellipses denote the contribution from higher excited states of the nucleon which decay faster than the ground state and first-excited state. We extract the ground state matrix element by performing a two-state combined fit with $C^{\rm 2pt}(P_z, t_{\rm sep})$ and the ratio $R_\Gamma(z, P_z, t_{\rm sep}, t) = C^{\rm 3pt}_\Gamma(z, P_z, t_{\rm sep}, t)/C^{\rm 2pt}(P_z, t_{\rm sep})$. Details of the fit can be found in Supplemental Material [39].

TABLE I. The simulation setup, including lattice spacing a, lattice size $L^3 \times T$, and the pion masses [47]. The parameters of X650 are exactly the same as A654 [48], except that X650's spatial volume is 8 times that of A654. For more details, we refer the interested readers to Table II in Supplemental Material [39]. For zero-momentum matrix elements, the numbers of configurations used are reduced to 350 for H102, and 100 for H105 and N203, because that already gives a satisfactory signal-to-noise ratio.

Ensemble	a (fm)	$L^3 \times T$	m_π (MeV)	$m_\pi L$	$N_{\rm conf}$
X650	0.098	$48^3 \times 48$	338	8.1	1500
H102	0.085	$32^3 \times 96$	354	4.9	500
H105	0.085	$32^3 \times 96$	281	3.9	500
C101	0.085	$48^3 \times 96$	222	4.6	500
N203	0.064	$48^3 \times 128$	348	5.4	500
N302	0.049	$48^3 \times 128$	348	4.2	500

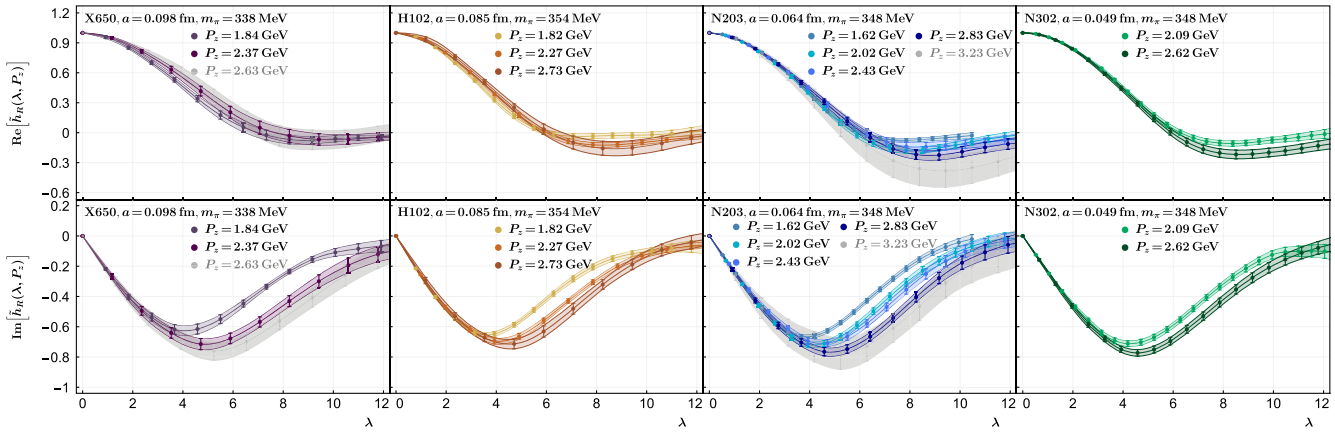

FIG. 2. The real (top) and imaginary (bottom) parts of the renormalized matrix elements for different ensembles as functions of λ at scale $\mu = 2$ GeV.

In Fig. 2, we plot the renormalized quasi-LF correlation in the hybrid scheme, as a function of the quasi-LF distance $\lambda = zP_z$. Note that our normalized quasi-LF correlation has the advantage that the one-loop logarithms in the chiral extrapolation [see Eq. (7) below] will get partially canceled. The data points are obtained on ensembles with nearly the same pion mass. As can be seen from the figure, the results show a good convergence as P_z increases for all ensembles. However, as we increase the nucleon boost momentum, the excited-state contamination worsens so that uncertainties increase. The $P_z = 2.63$ GeV data on X650 and $P_z = 3.23$ GeV data on N203 have much larger uncertainties compared to other datasets due to the relatively larger momentum on these ensembles. We exclude them in our analysis below. In Fig. 3, we show the pion mass dependence of the renormalized quasi-LF correlations on ensembles with the same lattice spacing $a = 0.085$ fm, where the pion masses are $m_\pi = \{354, 281, 222\}$ MeV, respectively. As shown in the figure, the results exhibit only a very mild dependence on the pion mass.

From the figures above, we can see that the uncertainty of the renormalized quasi-LF correlation grows at large distance, while a Fourier transform to momentum space requires the quasi-LF correlation at all distances. If we do a brute-force truncation and Fourier transform, unphysical oscillations will appear in the momentum space distribution. To resolve this issue, we adopt a physics-based extrapolation form [29] at large quasi-LF distance:

$$H_m^R(z, P_z) = \left[\frac{c_1}{(i\lambda)^a} + e^{-i\lambda}\frac{c_2}{(-i\lambda)^b}\right] e^{-\lambda/\lambda_0}, \qquad (6)$$

where the algebraic terms in the square bracket account for a power law behavior of the transversity PDFs in the end point region and the exponential term comes from the expectation that at finite momentum the correlation function has a finite correlation length (denoted as λ_0) [29], which becomes infinite when the momentum goes to infinity. The detail of the extrapolation is expected to affect the final results in the small- and large-x region where LaMET expansion breaks down [28]. An example of the extrapolation is given in Supplemental Material [39].

After the renormalization and extrapolation, we can Fourier transform the quasi-LF correlation to momentum space and extract the transversity PDF by applying perturbative matching. The transversity PDF extracted this way still contains lattice artifacts which shall be removed by performing a continuum extrapolation. Also, our calculations are not done at infinite momentum and the physical point, so we have to extrapolate to infinite

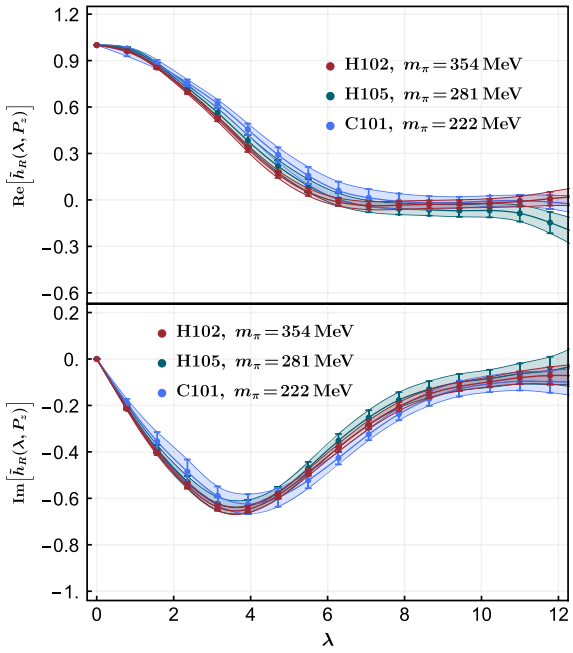

FIG. 3. The pion mass dependence of the real (top) and imaginary (bottom) part of the renormalized matrix elements for different ensembles with the same lattice spacing $a = 0.085$ fm and momentum $P_z = 1.82$ GeV.

momentum and physical pion mass. To this end, we perform a simultaneous extrapolation using the following functional form including a, P_z, and m_π:

$$\delta q(x, P_z, a, m_\pi) = \frac{1 - g' m_\pi^2 \ln(m_\pi^2/\mu_0^2) + m_\pi^2 k(x)}{1 - g' m_\pi^2 \ln(m_\pi^2/\mu_0^2)} \times \left[\delta q_0(x) + a^2 f(x) + a^2 P_z^2 h(x) + \frac{g(x,a)}{P_z^2}\right], \quad (7)$$

where $\delta q(x, P_z, a, m_\pi)$ on the lhs denotes the transversity PDF results obtained in our calculation on different ensembles. The extrapolation of the pion mass dependence follows from the study in Ref. [49] (with $\mu_0 = 1$ GeV and $g' = -(4g_A^2 + 1)/[2(4\pi f_\pi)^2]$ and g_A the axial charge of the nucleon) and for the CLS ensembles in Ref. [50]. The $a^2 f(x)$ term denotes the leading discretization error which begins at $\mathcal{O}(a^2)$ as the lattice action is already $\mathcal{O}(a)$ improved. The $a^2 P_z^2$ term represents the momentum-dependent discretization error. The last term in the square bracket accounts for the leading higher-twist contribution, where in the numerator we also include a potential a dependence. Choosing $g(x, a)$ as a generic function or parametrizing it with a quadratic form in a yields similar results with slightly different errors. We refer the readers to Supplemental Material [39] for details of this extrapolation. Eventually, the desired transversity PDF is given by

$$\delta q(x) = \frac{1 - g' m_{\pi,\mathrm{phys}}^2 \ln(m_{\pi,\mathrm{phys}}^2/\mu_0^2) + m_{\pi,\mathrm{phys}}^2 k(x)}{1 - g' m_{\pi,\mathrm{phys}}^2 \ln(m_{\pi,\mathrm{phys}}^2/\mu_0^2)} \times \delta q_0(x), \quad (8)$$

where $m_{\pi,\mathrm{phys}} = 135$ MeV.

The fitting to extract bare matrix elements, the hybrid renormalization, large-λ extrapolation, Fourier transformation, and combined extrapolation are performed based on 4000 bootstrap resampled two-point and three-point correlators.

Numerical result.—Our final result for the physical isovector quark transversity PDF $\delta u(x) - \delta d(x)$ (normalized by nucleon isovector tensor charge g_T) is shown in Fig. 4, together with the results of recent global analyses from the JAM Collaboration (JAM20 [18] and JAM22 [6]). JAM20 is the global analysis that finds, for the first time, agreement between phenomenology and lattice calculation of all nucleon tensor charges $\delta u, \delta d$ and the isovector combination g_T. JAM22 provides an update to JAM20 by including certain new datasets and constraints from the Soffer bound and lattice g_T result. Given the sensitivity of the results to the choice of datasets, we tend to view the difference between the two curves as an indication of systematic uncertainties from global fits. As can be seen from the figure, our result lies between the two global analyses and agrees with both within $1 - 2\sigma$ error. Note that we have plotted two shaded bands at the end point regions to indicate that LaMET predictions are not reliable there (taken as $x \in [-0.1, 0.1]$ and $x \in [0.9, 1]$), which are estimated from the observation that the higher-twist terms in LaMET factorization Eq. (4) are of $\mathcal{O}(1)$, i.e., $\Lambda_{\mathrm{QCD}}/(xP_z) \sim 1$ and $\Lambda_{\mathrm{QCD}}/[(1-x)P_z] \sim 1$ with the highest momentum in this Letter $P_z = 2.83$ GeV. This estimation is consistent with the recent approach incorporating the renormalization group resummation procedure [51], as can be seen from Supplemental Material [39]. Our error band includes both statistical and systematic uncertainties, where the latter have four different sources. The first is the renormalization scale dependence, which is estimated by varying the scale to 3 GeV. The second error comes from the extrapolation to continuum, infinite momentum, and physical mass, which is relatively small. The third error is from the choice of z_s in the hybrid renormalization scheme. We choose $z_s = 0.3$ fm, vary it down to $z_s = 0.18$ fm, and take the difference as a systematic error. Lastly, the large λ extrapolation also introduces some error that mainly affects the small-x region $-0.2 \lesssim x \lesssim 0.2$. We have chosen different regions to do the extrapolation to estimate this error. More details of the systematic uncertainties can be found in Supplemental Material [39].

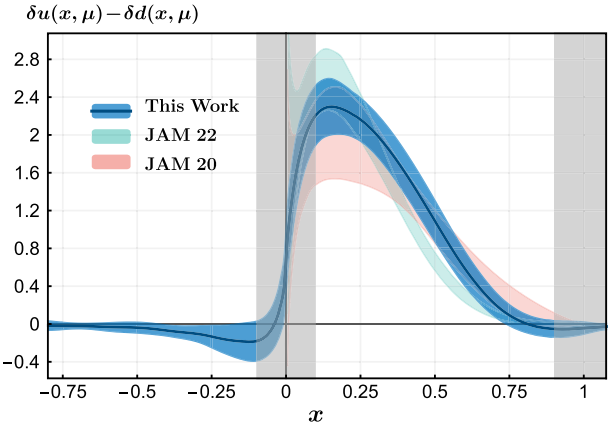

FIG. 4. Our final proton isovector transversity PDF at renormalization scale $\mu = 2$ GeV, extrapolated to the continuum, physical pion mass, and infinite momentum limit ($a \to 0, m_\pi \to m_{\pi,\mathrm{phys}}, P_z \to \infty$), compared with JAM20 [18] and JAM22 [6] global fits. All results are normalized to the nucleon isovector tensor charge g_T. The blue error band includes both statistical and systematic errors. The vertical light gray bands denote the end point regions where LaMET predictions are not reliable.

In the negative-x region, our result is consistent with zero, which puts a strong constraint on the sea flavor asymmetry. JAM plans to update their global analysis by including spin asymmetry data from STAR [6]. It will be very interesting to see how their new analysis compares with our lattice result.

Summary.—We present a state-of-the-art calculation of the isovector quark transversity PDF with LaMET.

The calculation is done at various lattice spacings, pion masses, and large nucleon momenta and extrapolated to the continuum, physical mass, and infinite momentum limit. With high statistics, we have performed multistate analyses with multiple source-sink separations to remove the excited-state contamination and applied state-of-the-art renormalization, matching, and extrapolation. Our result provides the most reliable lattice prediction of the isovector quark transversity PDF in the proton so far and will offer guidance to measurements at JLab and EIC.

We thank the CLS Collaboration for sharing the lattices used to perform this study. We are grateful to Wolfgang Söldner for helpful discussions on the X650 ensemble and Daniel Pitonyak and Nobuo Sato for providing the JAM fits data of the transversity PDF. We also thank Yu-Sheng Liu and Yong Zhao for helpful correspondence. A. S. thanks the University of the Basque Country, Bilbao for hospitality. This work was supported in part by the High Performance Computing Center of Central South University. The authors gratefully acknowledge the Gauss Centre for Supercomputing e.V. for funding this project by providing computing time on the GCS Supercomputer SuperMUC at Leibniz Supercomputing Centre. The LQCD calculations were performed using the multigrid algorithm [52,53] and Chroma software suite [54]. X. X. is supported in part by the National Natural Science Foundation of China under Grants No. 12275364 and No. 11905296. Y. Y. is supported in part by the National Natural Science Foundation of China under Grant No. 12293060, No. 12293062 and No. 12047503 and the Strategic Priority Research Program of Chinese Academy of Sciences, Grants No. XDB34030303 and No. YSBR-101. F. Y., L. M., and J.-H. Z. are supported in part by the National Natural Science Foundation of China under Grants No. 11975051 and No. 12375080. A. S., H.-T. S., P. S., Y. Y., and J.-H. Z. are also supported by a NSFC-DFG joint grant under Grant No. 12061131006 and SCHA 458/22. P. S. is also supported by Strategic Priority Research Program of the Chinese Academy of Sciences under Grant No. XDB34030301. X. J. is supported by the U.S. Department of Energy, Office of Science, Office of Nuclear Physics, under Contract No. DE-SC0020682. J.-W. C. is supported by the Taiwan Ministry of Science and Technology under Grant No. 111-2112-M-002-017 and the Kenda Foundation. J. H. is supported by National Natural Science Foundation of China under Grant No. 12205106 and Guangdong Major Project of Basic and Applied Basic Research No. 2020B0301030008.

*Corresponding author: pengsun@impcas.ac.cn
†Corresponding author: xnxiong@csu.edu.cn

[1] J. P. Ralston and D. E. Soper, Nucl. Phys. **B152**, 109 (1979).
[2] R. L. Jaffe and X. D. Ji, Phys. Rev. Lett. **67**, 552 (1991).
[3] R. L. Jaffe and X. D. Ji, Nucl. Phys. **B375**, 527 (1992).
[4] J. L. Cortes, B. Pire, and J. P. Ralston, Z. Phys. C **55**, 409 (1992).
[5] R. L. Jaffe and X. D. Ji, Phys. Rev. Lett. **71**, 2547 (1993).
[6] L. Gamberg, M. Malda, J. A. Miller, D. Pitonyak, A. Prokudin, and N. Sato (Jefferson Lab Angular Momentum (JAM) Collaboration), Phys. Rev. D **106**, 034014 (2022).
[7] M. Constantinou, A. Courtoy, M. A. Ebert, M. Engelhardt, T. Giani, T. Hobbs, T. J. Hou, A. Kusina, K. Kutak, J. Liang *et al.*, Prog. Part. Nucl. Phys. **121**, 103908 (2021).
[8] M. Anselmino, M. Boglione, U. D'Alesio, A. Kotzinian, F. Murgia, A. Prokudin, and C. Turk, Phys. Rev. D **75**, 054032 (2007).
[9] M. Anselmino, M. Boglione, U. D'Alesio, A. Kotzinian, F. Murgia, A. Prokudin, and S. Melis, Nucl. Phys. B, Proc. Suppl. **191**, 98 (2009).
[10] M. Anselmino, M. Boglione, U. D'Alesio, S. Melis, F. Murgia, and A. Prokudin, Phys. Rev. D **87**, 094019 (2013).
[11] Z. B. Kang, A. Prokudin, P. Sun, and F. Yuan, Phys. Rev. D **91**, 071501(R) (2015).
[12] Z. B. Kang, A. Prokudin, P. Sun, and F. Yuan, Phys. Rev. D **93**, 014009 (2016).
[13] A. Bacchetta, A. Courtoy, and M. Radici, Phys. Rev. Lett. **107**, 012001 (2011).
[14] A. Bacchetta, A. Courtoy, and M. Radici, J. High Energy Phys. 03 (**2013**) 119.
[15] M. Radici, A. Courtoy, A. Bacchetta, and M. Guagnelli, J. High Energy Phys. 05 (**2015**) 123.
[16] H. W. Lin, W. Melnitchouk, A. Prokudin, N. Sato, and H. Shows, Phys. Rev. Lett. **120**, 152502 (2018).
[17] M. Radici and A. Bacchetta, Phys. Rev. Lett. **120**, 192001 (2018).
[18] J. Cammarota, L. Gamberg, Z. B. Kang, J. A. Miller, D. Pitonyak, A. Prokudin, T. C. Rogers, and N. Sato (Jefferson Lab Angular Momentum Collaboration), Phys. Rev. D **102**, 054002 (2020).
[19] V. Braun and D. Müller, Eur. Phys. J. C **55**, 349 (2008).
[20] X. Ji, Phys. Rev. Lett. **110**, 262002 (2013).
[21] X. Ji, Sci. China Phys. Mech. Astron. **57**, 1407 (2014).
[22] Y. Q. Ma and J. W. Qiu, Phys. Rev. Lett. **120**, 022003 (2018).
[23] H. W. Lin, E. R. Nocera, F. Olness, K. Orginos, J. Rojo, A. Accardi, C. Alexandrou, A. Bacchetta, G. Bozzi, J. W. Chen *et al.*, Prog. Part. Nucl. Phys. **100**, 107 (2018).
[24] A. V. Radyushkin, Phys. Rev. D **96**, 034025 (2017).
[25] C. Alexandrou, K. Cichy, M. Constantinou, K. Jansen, A. Scapellato, and F. Steffens, Phys. Rev. D **98**, 091503(R) (2018).
[26] Y. S. Liu, J. W. Chen, L. Jin, R. Li, H. W. Lin, Y. B. Yang, J. H. Zhang, and Y. Zhao, arXiv:1810.05043.
[27] C. Egerer *et al.* (HadStruc Collaboration), Phys. Rev. D **105**, 034507 (2022).
[28] X. Ji, Y. Liu, Y. S. Liu, J. H. Zhang, and Y. Zhao, Rev. Mod. Phys. **93**, 035005 (2021).
[29] X. Ji, Y. Liu, A. Schäfer, W. Wang, Y. B. Yang, J. H. Zhang, and Y. Zhao, Nucl. Phys. **B964**, 115311 (2021).
[30] Y. K. Huo *et al.* (Lattice Parton Collaboration (LPC)), Nucl. Phys. **B969**, 115443 (2021).
[31] J. W. Chen, X. Ji, and J. H. Zhang, Nucl. Phys. **B915**, 1 (2017).
[32] T. Izubuchi, X. Ji, L. Jin, I. W. Stewart, and Y. Zhao, Phys. Rev. D **98**, 056004 (2018).

[33] C. Alexandrou, K. Cichy, M. Constantinou, K. Hadjiyiannakou, K. Jansen, H. Panagopoulos, and F. Steffens, Nucl. Phys. **B923**, 394 (2017).
[34] A. Radyushkin, Phys. Rev. D **98**, 014019 (2018).
[35] V. M. Braun, A. Vladimirov, and J. H. Zhang, Phys. Rev. D **99**, 014013 (2019).
[36] Z. Y. Li, Y. Q. Ma, and J. W. Qiu, Phys. Rev. Lett. **122**, 062002 (2019).
[37] T. Harris, G. von Hippel, P. Junnarkar, H. B. Meyer, K. Ottnad, J. Wilhelm, H. Wittig, and L. Wrang, Phys. Rev. D **100**, 034513 (2019).
[38] Y. Aoki *et al.* (Flavour Lattice Averaging Group (FLAG)), Eur. Phys. J. C **82**, 869 (2022).
[39] See Supplemental Material at http://link.aps.org/supplemental/10.1103/PhysRevLett.131.261901 for the details of self-renormalization procedure, extraction of nucleon isovector tensor charge, one-loop matching, additional information of lattice data analysis, including the fitting strategy, large extrapolation and combined extrapolation to continuum limit, physical pion mass and large momentum limit. The uncertainty analysis and details of applying renormalization group resummation for the end-point region is also provided in the Supplemental Material.
[40] S. Park, R. Gupta, B. Yoon, S. Mondal, T. Bhattacharya, Y. C. Jang, B. Joo, and F. Winter (Nucleon Matrix Elements (NME) Collaboration), Phys. Rev. D **105**, 054505 (2022).
[41] M. Abramczyk, T. Blum, T. Izubuchi, C. Jung, M. Lin, A. Lytle, S. Ohta, and E. Shintani, Phys. Rev. D **101**, 034510 (2020).
[42] N. Hasan, J. Green, S. Meinel, M. Engelhardt, S. Krieg, J. Negele, A. Pochinsky, and S. Syritsyn, Phys. Rev. D **99**, 114505 (2019).
[43] V. M. Braun, Y. Ji, and A. Vladimirov, J. High Energy Phys. 10 (**2021**) 087.
[44] C. Y. Chou and J. W. Chen, Phys. Rev. D **106**, 014507 (2022).
[45] G. S. Bali, B. Lang, B. U. Musch, and A. Schäfer, Phys. Rev. D **93**, 094515 (2016).
[46] M. Bruno, D. Djukanovic, G. P. Engel, A. Francis, G. Herdoiza, H. Horch, P. Korcyl, T. Korzec, M. Papinutto, S. Schaefer *et al.*, J. High Energy Phys. 02 (**2015**) 043.
[47] Gunnar S. Bali, J. High Energy Phys. 05 (**2023**) 035..
[48] T. Bhattacharya, S. D. Cohen, R. Gupta, A. Joseph, H. W. Lin, and B. Yoon, Phys. Rev. D **89**, 094502 (2014).
[49] J. W. Chen and X. d. Ji, Phys. Lett. B **523**, 107 (2001).
[50] G. S. Bali *et al.* (RQCD Collaboration), Eur. Phys. J. A **55**, 116 (2019).
[51] Y. Su, J. Holligan, X. Ji, F. Yao, J. H. Zhang, and R. Zhang, Nucl. Phys. **B991**, 116201 (2023).
[52] R. Babich, J. Brannick, R. C. Brower, M. A. Clark, T. A. Manteuffel, S. F. McCormick, J. C. Osborn, and C. Rebbi, Phys. Rev. Lett. **105**, 201602 (2010).
[53] J. C. Osborn, R. Babich, J. Brannick, R. C. Brower, M. A. Clark, S. D. Cohen, and C. Rebbi, Proc. Sci., LATTICE2010 (**2010**) 037 [arXiv:1011.2775].
[54] R. G. Edwards and B. Joó (SciDAC, LHPC and UKQCD Collaborations), Nucl. Phys. B, Proc. Suppl. **140**, 832 (2005).